A Letters Journal Exploring the Frontiers of Physics

March 2020

EPL, **129** (2020) 50001 www.epljournal.org
doi: 10.1209/0295-5075/129/50001

A cardiodynamic model for power laws of heartbeats in aging and congestive heart failure

S. Li[1], R. Lin[1], A. C. Beki[2(a)], C. Wang[3(b)] and X. Zhang[4(c)]

[1] *School of Electronic Science and Engineering, Ministry of Education Key Laboratory of Modern Acoustics, Nanjing University - Nanjing 210023, China*
[2] *Research Institute of Biomedical Engineering, Nanjing University - Nanjing 210023, China*
[3] *Nanjing University of Posts and Telecommunications - Nanjing 210003, China*
[4] *School of Electronic Science and Engineering, Nanjing University - Nanjing 210023, China*

received 5 November 2019; accepted in final form 2 March 2020
published online 31 March 2020

PACS 05.45.Tp – Time series analysis
PACS 87.19.Hh – Cardiac dynamics
PACS 87.10.Ed – Ordinary differential equations (ODE), partial differential equations (PDE), integro-differential models

Abstract – The output of a healthy physiological system exhibits complex fluctuation. Nonlinear analysis, such as power-law characteristics, shows the potential for detecting changes in the biological complexity of disease and aging. This paper characterized the heart rate variability (HRV) of aging and patients with congestive heart failure (CHF) by three types of distribution: Zipf's law, Heaps' law, and frequency distribution. All data analysis and modeling are based on a constructed sequence, that is, the monotonous increase to monotonous decrease amplitude ratios as derived from heartbeat interval data. The experimental result shows a significant decrease of HRV from healthy young people to healthy elderly to CHF patients. We proposed a model by taking account of the "rich-get-richer" theory in experimental observations, which successfully reproduced three types of distribution characterizing the constructed ratio sequences as obtained from the analysis of measured cardiac data. This work provides insight into the dynamic mechanism of cardiac data underlying the regulation of autonomic nerve.

Introduction. – Heart rate variability (HRV) is a commonly used quantitative indicator for judging autonomic nerve function. It refers to the difference between successive heartbeat cycles [1,2]. The cardiac cycle changes irregularly as the pacing of the sinoatrial node is coordinated by both sympathetic and parasympathetic nerves, which will cause cardiac acceleration and attenuation, respectively [3–5]. In a nutshell, the higher the heart rate variability, the better the body can adapt to internal and external influences. Conversely, it may imply serious health diseases [6–9]. Researches have shown that autonomic nerve activity declines in healthy people over the age of 70, whose HRV is correspondingly lower than healthy young adults' one [10–12]; patients with CHF also experience a significantly decreased HRV due to their chronically excited sympathetic nerve [13–16]. In addition to its value in screening for heart disease, HRV owns broad application prospects in the diagnosis of diseases such as Parkinson's [17], hypertension [18], diabetes [19], epilepsy [20] and so on.

Numerous linear methods of calculating HRV have emerged. Time domain analysis based on RR intervals is used to calculate parameters like SDNN (the standard deviation of the normal-to-normal intervals) and rMSSD (the root mean square successive difference of intervals), where rMSSD can effectively assess parasympathetic nervous activity [21]. Frequency domain methods study the distribution of HRV energy varying with frequency. They perform a fast Fourier transform [22] or autoregression for continuous RR interval values to obtain the heart rate function spectrum. The frequency component of power spectrum density (PSD) can be used to monitor autonomic nervous function [23]: 1) HF (high frequency, 0.15–0.4 Hz) works to represent parasympathetic nervous activity, 2) LF (low frequency, 0.04–0.15 Hz) is confirmed to be associated with baroreflex sensitivity [24,25], and 3) LF/HF reflects the

(a) E-mail: a.beki@hotmail.com
(b) E-mail: cheng.li_wang@hotmail.com
(c) E-mail: zhxg@nju.edu.cn

balance of sympathovagal nervous system, while the output of a normal human heartbeat fluctuates in complex ways even at rest. The electrical activity of the heart is so highly nonlinear that linear methods are not sufficient to reveal its properties. Nonlinear analysis (*i.e.*, approximate entropy [26], detrended fluctuation analysis [27]) is now widely accepted to describe the biological system dynamics in a more efficient manner and shows potential in providing reliable prognostic information in disease stratification.

In this paper we did data analysis and modeling based on the constructed sequences, that is, the monotonous increase to monotonous decrease amplitude ratios as derived from heartbeat interval data. With these ratio sequences, we can observe the alternation of the increase and decrease of heart rate due to the sympathetic and parasympathetic nerve regulation. We aimed to evaluate cardiac risk and monitor the aging process by three types of power-law distribution: Zipf's law on frequency [28], Heaps' law on the growth of distinct values [29] and frequency distribution analysis. Zipf's law was originally proposed as the law of word frequency distribution, which can be expressed as: in the corpus of natural language, the word frequency $Z(r)$ is inversely proportional to its ranking r on the frequency table. Heaps' law describes how the number of distinct words $N(t)$ in a document grows with the document length t. Besides, in this work, an original model was built by considering the "rich-get-richer" theory in experimental observations to infer the cardiac dynamics under autonomic regulation. It is shown that the model reproduces three types of distribution characterizing these ratio sequences as obtained from the analysis of measured cardiac data.

Methods and result. –

Data and preprocessing. The ECG signals used herein come from the Physiobank Archives, where data of healthy people are from the Fantasia database and CHF patients' data are from the BIDMC Congestive Heart Failure Database [30].

The MIT-BIH Fantasia database contains long-term ECG recordings of 19 healthy young people (aged 21–34) and 15 healthy elderly people (aged 68–85). All subjects were asked to rest at sinus rhythm while watching the Disney movie Fantasia (1940) to help maintain their awareness. The ECG signals were collected at 250 Hz for 2 h. The BIDMC CHF database contains long-term ECG recordings of 14 people (aged 22–71) with severe congestive heart failure (NYHA 3–4). Each recording includes a 20 hour dual lead ECG signal and was sampled at 250 Hz. The original analog electrical signal was recorded by a dynamic ECG recorder with a bandwidth of 0.1 Hz–40 Hz [30]. To ensure accuracy, the heart rate data was detected with an Arrhythmia Automatic Detection Algorithm and additional manual checks. The timestamp of the R-wave peak was automatically detected using an algorithm provided by the database.

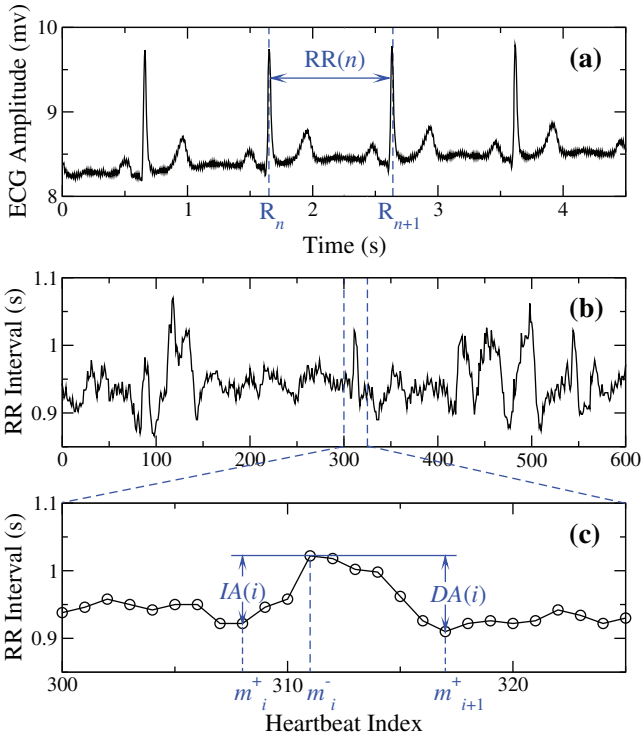

Fig. 1: The construction process of heart rate related time sequence $AR(i)$. (a) is a segment of the ECG signal. (b) shows the $RR(n)$ sequence extracted from an ECG signal. (c) illustrates the calculation of $IA(i)$ and $DA(i)$ that make up the $AR(i)$ sequence.

Based on the variation trend of heartbeat, we constructed a ratio sequence $AR(i)$ (fig. 1), which will be used for the further power-law analysis. Figure 1(a) is a segment of the ECG signal, where $RR(n)$ is the time interval between two adjacent R peaks. Figure 1(b) shows the $RR(n)$ sequence extracted from an ECG signal. Figure 1(c) marks the two components that make up the $AR(i)$ sequence (eq. (1)). Monotonously increased RR interval during $IA(i)$ phase indicates a decrease in heart rate, which is caused by enhanced parasympathetic activity. Correspondingly, the $DA(i)$ phase represents an increase in both heart rate and sympathetic regulation.

$$AR(i) = \frac{IA(i)}{DA(i)} = \frac{RR(m_i^-) - RR(m_i^+)}{RR(m_i^-) - RR(m_{i+1}^+)}. \quad (1)$$

The construction of $AR(i)$ reflects the change of autonomic nerve regulation, therefore, we think the analysis of this ratio sequence has a certain physiological basis as describing the complexity of cardiac data.

Power law analysis of $AR(i)$ sequence. We first carried out a frequency distribution analysis of $AR(i)$. $n(k)$ in eq. (2) represents the number of $AR(i)$ values

Table 1: Statistical result of the power-law exponents. Significant intergroup differences are indicated by β (probability distribution, fitting range $k \in [1, max]$), α (Zipf's law, fitting range $r \in [10, 100]$), and λ (Heaps' law, fitting range $t \in [100, max]$).

Scaling exponent	Young ave. ± std. dev.	Elderly ave. ± std. dev.	CHF ave. ± std. dev.
β	2.48 ± 0.48	1.76 ± 0.29	1.19 ± 0.18
α	0.56 ± 0.18	1.03 ± 0.38	2.37 ± 1.05
λ	0.75 ± 0.11	0.59 ± 0.12	0.39 ± 0.12

that occur k times,

$$P(k) = \frac{n(k)}{\sum_k n(k)}. \tag{2}$$

It can be found in all groups that the probability distribution $P(k)$ of frequency k follows a power-law with exponent β (fig. 2(a)),

$$P(k) \sim k^{-\beta}. \tag{3}$$

However, statistically, these groups show significant difference under Student's t-test ($p < 0.01$): young people $\beta_y = 2.48 \pm 0.48$, elderly $\beta_e = 1.76 \pm 0.29$, patients with CHF $\beta_c = 1.19 \pm 0.18$ (fitting range $k \in [1, max]$) (table 1).

We next perform Zipf's rank analysis, sorting the frequency of distinct $AR(i)$ values in descending order to obtain the corresponding Zipf's plot. This shows that the frequency $Z(r)$ exhibits a power-law behavior as a function of the rank r characterized by a scaling exponent α,

$$Z(r) \sim r^{-\alpha}. \tag{4}$$

$Z(r)$ is the normalized frequency ($Z = k/N$, N is the total length of sequence $AR(i)$). To promote the intuitiveness of comparison between each group, the result curves of young people (blue circle) and CHF patients (red triangle) in fig. 2(b) were shifted up and down, respectively. Result reveals that Zipf's curve of all groups turns at $r \approx 10$. In the high-frequency region $r \in [2, 10]$, the distribution trend is similar for all groups. By fitting all values in this region, $\alpha = 0.54$ can be obtained. In the low-frequency region $r \in [10, 100]$, the three curves show obviously different degrees of transition. The fitting result of this interval reveals significant intergroup differences ($p < 0.01$) (table 1): young people $\alpha_y = 0.56 \pm 0.18$, elderly $\alpha_e = 1.03 \pm 0.38$, CHF patients $\alpha_c = 2.37 \pm 1.05$.

Additionally, we found that the growth of distinct values in sequence $AR(i)$ conforms to Heaps' law

$$N(t) \sim t^{\lambda}, \tag{5}$$

where $N(t)$ is the number of distinct values in an instance sequence of size t. Figure 2(c) shows the Heaps-law plot,

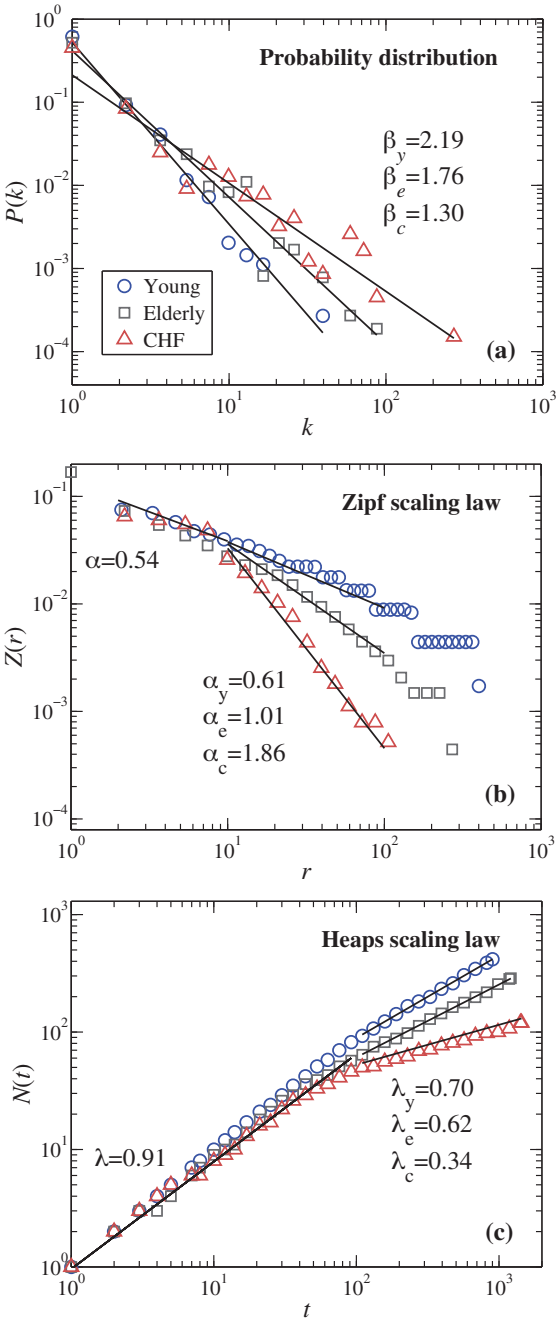

Fig. 2: Power-law analysis results for one subject in each group, in which (a) is a probability distribution, (b) is Zipf's law, and (c) is Heaps' law. In the Zipf plot, curves of young people and CHF patients were shifted up and down, respectively, to promote comparison. Straight lines indicate the fitting range. Turning point of (b) and (c) appears at $r = 10$ and $t = 100$, respectively.

and each group exhibits different degrees of curvature at $t \approx 100$. In size $t \in [1, 100]$, the number of distinct $AR(i)$ values in each group maintains a similar growth trend $\lambda = 0.91$, while as the length of the sequence increases, a significant difference ($p < 0.01$) appears in $t \in [100, max]$: young people $\lambda_y = 0.75 \pm 0.11$, elderly $\lambda_e = 0.59 \pm 0.12$, CHF patients $\lambda_c = 0.39 \pm 0.12$ (table 1).

Modeling and simulation of cardiac dynamics. In the language system, the Yule-Simon model [31,32] describes text generation with the "rich-get-richer" theory, which means that a word appearing more frequently will have a higher probability to be copied. This theory also contributes to a power-law frequency distribution and Zipf's law. Our work combines empirical observations with the Yule-Simon model to derive analytical solutions of the power-law phenomenons above.

We modeled the generation of $AR(i)$ sequence as follows:

i) a new value is added to the sequence with probability p,

ii) an appeared value is randomly chosen and copied with probability $1-p$.

Think of p as the slope of the Heaps' plot at time t, that is, the growth rate of the curve. Neglecting the difference in the shorter size region $t \in [1, 100]$, for $t \in [100, max]$, the generation dynamics can be obtained through the power-law relationship between N_t and t (fig. 2(c)),

$$\frac{\mathrm{d}N_t}{\mathrm{d}t} = p = a_0 t^{-a_1}. \tag{6}$$

Integrating eq. (6) with boundary condition $N_0 = 0$, a power function of N_t can be obtained

$$N_t = \frac{a_0 t^{1-a_1}}{1-a_1}. \tag{7}$$

According to the "rich-get-richer" theory, in step ii), the probability an appeared value is chosen depends on its frequency in existing sequence, that is, the more frequently a value appears, the more likely it will be chosen to add to the end of the sequence,

$$f(k) = \left(\frac{k(i)}{t}\right)^{a_2}, \tag{8}$$

where $k(i)$ is the number of occurrences of the value in an instance $AR(i)$ sequence of size t, and $f(k)$ is the probability of being chosen. Parameter a_2 represents the dependence of $f(k)$ on $k(i)$. Define $n(t,k)$ as the number of distinct values that appear k times until time t, then $N_t * p(k) = n(t,k)$. Obviously, we can get [33]

$$n(t+1,k+1) = n(t,k+1)[1-f(k+1)] + n(t,k)f(k). \tag{9}$$

Substitute eq. (8) into eq. (9), then

$$\begin{aligned} N_{t+1}p(k+1) &= N_t p(k+1)\left[1-\left(\frac{k+1}{t}\right)^{a_2}\right] \\ &\quad + N_t p(k)\left(\frac{k}{t}\right)^{a_2}. \end{aligned} \tag{10}$$

Substituting $p(k+1)-p(k) = \mathrm{d}p/\mathrm{d}k$, $N_{t+1}-N_t = \mathrm{d}N_t/\mathrm{d}t$, and eq. (6) into eq. (10), a differential equation can be obtained

$$\frac{\mathrm{d}p}{p} = \mathrm{d}k\left[-\frac{a_0 t^{a_2-a_1}}{N_t k^{a_2}} + 1 - \left(\frac{k+1}{k}\right)^{a_2}\right]. \tag{11}$$

By approximation, we can get the analytical expression of $p(k)$

$$\begin{aligned} p &= Be^{-A}k^{-[A(1-a_2)+a_2]}, \\ A &= \frac{a_0 t^{a_2-a_1}}{N_t(1-a_2)}, \end{aligned} \tag{12}$$

where B is the normalization factor. In eq. (12), the power-law relationship between p and k is consistent with the experimental results in fig. 1(a).

Calculate the definite integral of function $p(k)$ [33]

$$\begin{aligned} p(k>k_0) &= 1 - \int_{k_{min}}^{k_0} p(k)\mathrm{d}k \\ &= 1 - Be^{-A}\frac{k_0^m - k_{min}^m}{m}, \end{aligned} \tag{13}$$

where $m = 1-[A(1-a_2)+a_2]$, and k_{min} is the smallest frequency. According to $p(k_{max} > k_{min}) = 1$, it could be obtained that

$$B = \frac{e^A m}{k_{max}^m - k_{min}^m}. \tag{14}$$

There will be $p(k>k_0) * N_t$ values that appear more than k_0 times. Therefore, a value that appears k_0 times should be ranked at

$$r = 1 + \left(1 - Be^{-A}\frac{k_0^m - k_{min}^m}{m}\right)N_t. \tag{15}$$

Thus, a normalized frequency can be obtained

$$Z(r) = k_0/N = \left(\frac{\left(1-\frac{r-1}{N_t}\right)e^A m}{B} + k_{min}^m\right)^{1/m} \Big/ N, \tag{16}$$

where N is the total length of sequence $AR(i)$.

In the simulation, we considered combined data of the entire group, which is built by connecting the $AR(i)$ of all subjects within each group according to their serial number. The values of a_0, a_1, a_2 are confirmed by parameter optimization: Young $a_0 = 1.43$, $a_1 = 0.2$, $a_2 = 0.96$, Elderly $a_0 = 1.46$, $a_1 = 0.39$, $a_2 = 1.01$, CHF $a_0 = 1.05$, $a_1 = 0.4$, $a_2 = 0.95$. The comparison between simulation results and the experimental data on power-law distributions is shown in fig. 3. To promote the intuitiveness of comparison, the Zipf law plot of young people (blue circle) and CHF patients (red triangle) were shifted up and down, respectively.

Conclusion. – Previous studies have demonstrated that the mechanism for youth and health lies in physiological complexity. As the body ages or becomes ill, the physiological process will tend to become simpler. As a stable and reliable indicator, heart rate variability can indicate individual differences in autonomic regulatory flexibility. Low heart rate variability predicts autonomic dysfunction and is associated with a large number of chronic diseases. At present, most relevant studies focus on linear

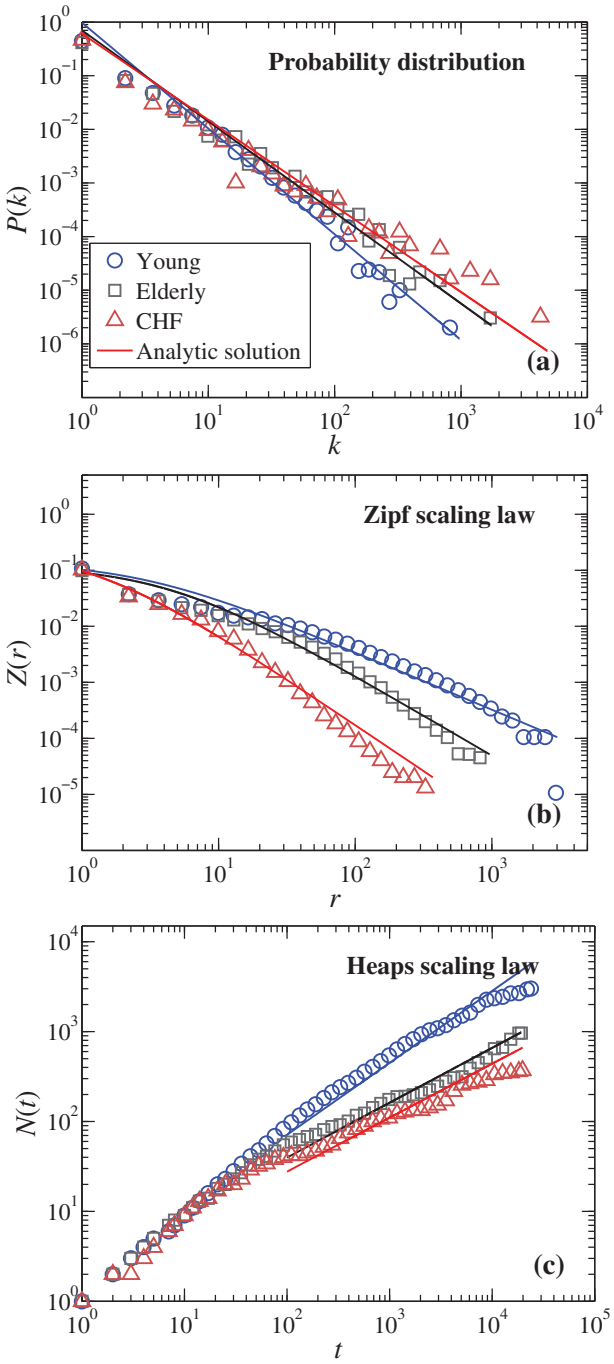

Fig. 3: Comparison between experimental data (symbols) and simulation results (lines) (combined data of all subjects within each group). (a) Probability distribution, (b) Zipf's analysis (curves of young people and CHF patients were shifted up and down, respectively, to promote comparison), and (c) Heaps' analysis.

analysis, which cannot fully reflect the nonlinear physiological process.

Differently from existing nonlinear methods, this work quantifies and models the mechanisms involved in cardiac data by scaling characteristics. Under the analysis of probability distribution, Zipf's law and Heaps' law, we hope to further understand the organization and dynamics of cardiac data. Thereinto, Heaps' law describes the growth of distinct values varying with system length, that is, the faster the number of distinct values grows, the more complex the sequence is. Specifically, exponent $\lambda_y > \lambda_e > \lambda_c$ implies that the HRV gradually decreases from healthy young people to healthy elderly to patients with CHF. This result is also consistent with previous research conclusions.

The innovation of this paper in the study of cardiac dynamics is 1) firstly embodied in the construction of $AR(i)$ sequence, which is based on the monotonous increase to monotonous decrease amplitude ratios as derived from RR interval data. With these ratio sequences, we can observe the alternation of the increase and decrease of heart rate due to the sympathetic and parasympathetic nerve regulation. 2) Secondly, the "rich-get-richer" mechanism, which plays an important role in the model construction, tells us that the autonomic nerve regulation of heart rate is not completely random, but biased. The model used to explain and reproduce the heartbeat dynamics has not been found in previous studies, and the agreement between simulation and experiment results also confirmed the conjecture in our model.

We hope the method and model proposed in this paper could help to better understand the regulation rules of autonomic nerve on cardiovascular system with physiological and physical foundation, and can be used for reference by relevant researchers in this area.

* * *

We acknowledge the support from the Fundamental Research Funds for the Central Universities of China, Priority Academic Program Development of Jiangsu Higher Education Institutions (PAPD), Graduate Interdisciplinary Innovation Research of Nanjing University (2017CL04).

REFERENCES

[1] Acharya U. R., Joseph K. P., Kannathal N., Lim C. M. and Suri J. S., *Med. Biol. Eng. Comput.*, **44** (2006) 1031.
[2] Kobayashi H., Ishibashi K. and Noguchi H., *Appl. Hum. Sci. J. Physiol. Anthropol.*, **18** (1999) 53.
[3] Floras J. S., *J. Am. Coll. Cardiol.*, **54** (2009) 375.
[4] Triposkiadis F., Karayannis G., Giamouzis G., Skoularigis J. and Butler J., *J. Am. Coll. Cardiol.*, **54** (2009) 1747.
[5] Esler M., *J. Appl. Physiol.*, **108** (2010) 227.
[6] Bitsios P., Prettyman R. J. and Szabadi E., *Age Ageing*, **25** (1996) 432.
[7] Tsuji H., Larson M. G., Venditti F. J., Manders E. S., Evans J. C. and Levy D., *Circulation*, **94** (1996) 2850.
[8] Panina G., Khot U. N., Nunziata E., Cody R. J. and Binkley P. F., *Am. Heart J.*, **131** (1996) 153.

[9] Szabo B. M., Van Veldhuisen D. J., Brouwer J. and Lie K. I., *Am. J. Cardiol.*, **76** (1995) 713.
[10] Pfeifer M., Weinberg C. R., Cook D. L., Best J. D., Reenan A. and Halter J. B., *Am. J. Med.*, **75** (1983) 249.
[11] Stein P. K., Barzilay J. I., Chaves P. H. M., Domitrovich P. P. and Gottdiener J. S., *Age Ageing*, **38** (2008) 212.
[12] Ng A. V., Callister R., Johnson D. A. and Seals D. R., *Hypertension*, **21** (1993) 498.
[13] Kaye D. M., Lefkovits J., Bergin P., Broughton A. and Esler M. D., *J. Am. Coll. Cardiol.*, **26** (1995) 1257.
[14] Hasking G. J., Esler M. D., Jennings G., Burton D. and Korner P. I., *Circulation*, **73** (1986) 615.
[15] Francis G. S., *Am. Heart J.*, **118** (1989) 642.
[16] Esler M. D. and Kaye D. M., *J. Cardiovasc. Pharmacol.*, **35** (2000) S1.
[17] Haapaniemi T., Pursiainen V., Korpelainen J., Huikuri H., Sotaniemi K. and Myllylä V., *J. Neurol. Neurosurg. Psychiatry*, **70** (2001) 305.
[18] Schroeder E. B., Liao D., Chambless L. E., Prineas R. J., Evans G. W. and Heiss G., *Hypertension*, **42** (2003) 1106.
[19] Risk M. R., Bril V., Broadbridge C. and Cohen A. M., *Diabetes Technol. Therapeutics*, **3** (2001) 63.
[20] Persson H., Ericson M. and Tomson T., *Seizure*, **16** (2007) 504.
[21] Kleiger E. M. D. R., Stein K. P. and Bigger J. T., *Ann. Noninvasive Electrocardiol.*, **10** (2005) 88.
[22] Malik M., *Ann. Noninvasive Electrocardiol.*, **1** (1996) 151.
[23] Sztajzel J., *Swiss Med. Weekly*, **134** (2004) 514.
[24] Moak J. P., Goldstein D. S., Eldadah B. A., Saleem A., Holmes C., Pechnik S. and Sharabi Y., *Heart Rhythm*, **4** (2007) 1523.
[25] Baumert M., Lambert G. W., Dawood T., Lambert E., Esler M. D., Mcgrane M., Barton D., Sanders P. and Nalivaiko E., *Am. J. Physiol. Heart Circ. Physiol.*, **297** (2009) H674.
[26] Pincus S. M. and Viscarello R. R., *Obstet. Gynecol.*, **79** (1992) 249.
[27] Huikuri H. V., Mäkikallio T. H., Peng C.-K., Goldberger A. L., Hintze U., Møller M. *et al.*, *Circulation*, **101** (2000) 47.
[28] Florence P. S. and Zipf G. K., *Econ. J.*, **60** (1950) 808.
[29] Heaps H. S., *Information Retrieval: Computational and Theoretical Aspects* (Academic Press, Inc., Orlando, Fla., USA) 1978.
[30] Goldberger A. L., Amaral L. A. N., Glass L., Hausdorff J. M., Ivanov P. C., Mark R. G., Mietus J. E., Moody G. B., Peng C. and Stanley H. E., *Circulation*, **101** (2000) 215.
[31] Simon H. A., *Biometrika*, **42** (1955) 425.
[32] Simkin M. V. and Roychowdhury V. P., *Phys. Rep.*, **502** (2011) 1.
[33] Lu L., Zhang Z. and Zhou T., *Sci. Rep.*, **3** (2013) 1082.